Psychoneuroendocrinology 109 (2019) 104387

Contents lists available at ScienceDirect

Psychoneuroendocrinology

journal homepage: www.elsevier.com/locate/psyneuen

In vivo magnetic resonance imaging reveals the effect of gonadal hormones on morphological and functional brain sexual dimorphisms in adult sheep

David André Barrière[a,b], Arsène Ella[a,c], Hans Adriaensen[a], Charles E. Roselli[d], Philippe Chemineau[a], Matthieu Keller[a,*]

[a] UMR Physiologie de la Reproduction et des Comportements, INRA/CNRS/Université de Tours/IFCE, Nouzilly, France
[b] Neurospin, CEA, Université Paris-Saclay, Gif-sur-Yvette, France
[c] MRC Cognition & Brain Science Unit, University of Cambridge, UK
[d] Oregon Health & Science University, Portland, USA

ARTICLE INFO

Keywords:
Sex differences
Sheep
Voxel-based morphometry
Resting state fMRI
Gonadectomy

ABSTRACT

Sex differences in the brain and behavior are produced by the perinatal action of testosterone, which is converted into estradiol by the enzyme aromatase in the brain. Although magnetic resonance imaging (MRI) has been widely used in humans to study these differences, the use of animal models, where hormonal status can be properly manipulated, is necessary to explore the mechanisms involved. We used sheep, a recognized model in the field of neuroendocrinology, to assess brain morphological and functional sex differences and their regulation by adult gonadal hormones. To this end, we performed voxel-based morphometry and a resting-state functional MRI approach to assess sex differences in gonadally intact animals. We demonstrated significant sex differences in gray matter concentration (GMC) at the level of the gonadotropic axis, *i.e.,* not only within the hypothalamus and pituitary but also within the hippocampus and the amygdala of intact animals. We then performed the same analysis one month after gonadectomy and found that some of these differences were reduced, especially in the hypothalamus and amygdala. By contrast, we found few differences in the organization of the functional connectome between males and females either before or after gonadectomy. As a whole, our study identifies brain regions that are sexually dimorphic in the sheep brain at the resolution of the MRI and highlights the role of gonadal hormones in the maintenance of these differences.

1. Introduction

Males and females show various sexually dimorphic traits in adulthood at the behavioral level that relate to the structure and function of the brain (McCarthy et al., 2015). Characterizing these sexual differences is of importance not only to gain a global understanding of the normal brain but also to gain insights into various brain disorders that are of differential prevalence and progression between males and females (Miller et al., 2017). Sex differences related to reproductive function are one of the most prominent types of sexual dimorphism, as both the neuroanatomical and functional organization of the gonadotropic axis differ widely between males and females.

In mammalian species, the classic view of sexual differentiation holds that these sex differences develop under the perinatal influence of testosterone and/or estradiol derived from the neural aromatization of testosterone (Alexander et al., 2011; Bakker and Baum, 2008). The brain develops as male in the presence of these hormones, and testicular testosterone in male embryos is necessary for the expression of male-typical hormonal and associated behavioral responses later in life, a process known as masculinization. Testosterone exposure not only masculinizes the brain but also actively defeminizes it so that males are unable to exhibit female-typical behavioral or physiological responses. By contrast, the absence of hormonal exposure predisposes animals to display female-typical adult sexual behaviors and hormone responses, a process known as feminization. While the early actions of sex steroids are necessary for the maturation and/or organization of several brain structures and neural circuits (Arnold, 2009), the differentiated neural circuits in adults are then responsible for sex-typical responses when sex steroids are synthesized by the mature gonad. Thus, the permanent developmental effects of sex steroids are usually referred to as “organizational”, while the transient or reversible effects observed during adulthood are referred to as “activational”.

* Corresponding author at: Laboratoire de Physiologie de la Reproduction et des Comportements, UMR 7247 INRA/CNRS/Université de Tours/IFCE, 37380, Nouzilly, France.
E-mail address: Matthieu.Keller@tours.inra.fr (M. Keller).

https://doi.org/10.1016/j.psyneuen.2019.104387
Received 29 January 2019; Received in revised form 19 July 2019; Accepted 22 July 2019

While these effects have been studied mostly in rodents, similar mechanisms exist in many other mammalian species. The sheep is an animal model that offers a unique opportunity to study brain mechanisms underlying sexual differentiation for several reasons, including the ability to perform long-term blood or cerebrospinal fluid sampling (Clarke and Cummins, 1982), the ability to manipulate the hormonal milieu in the fetus or adult (Clarke and Cummins, 1982; Perkins and Roselli, 2007) and the abundance of information that exists characterizing reproductive physiology and behavior in this species (for review Roselli and Stormshak, 2010, 2009a,b). Sexual differentiation of the sheep brain is dependent on testosterone and androgen receptor signalling during gestation (Cheng et al., 2010; Foster et al., 2002; Robinson et al., 1999; Roselli and Stormshak, 2010). While these studies, performed at the cellular or molecular levels, are very informative, they only examined a limited number of hypothalamic nuclei. Thus, information about other possible sexually dimorphic brain regions is lacking.

Magnetic resonance imaging (MRI) allows investigation at the level of the whole brain and has been widely used in humans to study sex differences in the function and organization of the brain (Burke et al., 2016, 2012). MRI is now a routine approach in neuroscience due to several advantages, including its noninvasive nature and the ability to perform longitudinal studies that allow changes within the same individuals to be tracked over time. However, due to ethical considerations, it is not possible to experimentally manipulate the hormonal milieu in humans, thus highlighting and reinforcing the usefulness of animal models such as sheep.

Some evidence suggests that gray and white matter content in sheep brain are sexually dimorphic, but because of the suboptimal resolution of the images and the lack of the appropriate neuroinformatic tools (namely, a brain template and atlas), the data could not be analyzed properly (Nuruddin et al., 2013). We recently established the tools necessary for conducting MRI experiments in sheep (Ella et al., 2017; Ella and Keller, 2015). In this study, we employed these tools to map and compare sexually dimorphic brain structures and connectivity in rams and ewes. This comparison was performed by using voxel-based morphometry (VBM) to assess neuroanatomical differences in gray matter concentrations (GMC) according to sex. We also validated resting-state functional MRI to assess basal dynamic activity differences between sexes. Finally, we tested which sex differences are programmed during sexual differentiation (organizational effect) or due to adult gonadal hormones (activational effect) by analyzing the effect of gonadectomy.

2. Materials and methods

2.1. Animals

Experiments were performed at the National Institute for Agronomic Research (Institut national pour la recherche agronomique, INRA) in Nouzilly, France (latitude 47°, 32 N and longitude 0°, 46E) on adult Ile-de-France sheep (*Ovis aries*). A total of 24 animals (4 years old) were used: 12 ewes (50.33 ± 0.71 kg) and 12 rams (70.91 ± 0.92 kg). Animals were maintained indoors during the experiment and were fed daily with barley straw, Lucerne hay and commercial concentrate and had access to water and mineral blocks *ad libitum*. All procedures were performed in accordance with the European directive 2010/63/EU for animal protection and welfare used for scientific purposes and approved by the local ethical committee for animal experimentation (CEEA VdL, Tours, France, authorization N° 10,465).

2.2. Experimental protocol

Animals were scanned twice in October and November 2017 at the CIRE platform (INRA Nouzilly, France, http://www.val-de-loire.inra.fr/cire). One week before the first scan, progesterone vaginal sponges (flugestone acetate, Chronogest CR 20 mg, MSD, Beaucouze, France) were placed in ewes to induce and maintain a luteal-like phase until the first day of the scan. On the day of the scan, sheep were weighed, and a blood sample was collected by jugular venipuncture to check the hormonal status of the animal. After the first scan, vaginal sponges were retrieved from the ewes, and both ewes and rams were gonadectomized following established procedures. To this end, the sheep were fasted 24 h before surgery. Following premedication with an i.v. injection of thiopental (14 mg/kg body weight, BW; Nesdonal, Merial, Villeurbanne, France), the sheep were intubated and maintained under anesthesia with a closed circuit of 3 to 4% isoflurane (Vetflurane, Virbac, Carros, France) and 100% oxygen. Castration and ovariectomy were conducted under sterile surgical conditions. Local anesthesia with lidocaine (4%, Lurocaïne, Vétoquinol, Luré, France) was given prior to scrotal incision in males and laparotomy in females. Testicles or ovaries were surgically extracted, and the tissues were sutured. The entire procedure was performed within 20 min. Postoperative ventilation with oxygen was maintained until the first signs of awakening appeared. The sheep were then housed individually for 6 h in a padded stall before being put back with congeners. They received an anti-inflammatory drug for 2 days (2 mg/kg BW flunixin meglumine, Finadyne®, Intervet, Beaucouzé, France), an antiedema medication: (1 mg/kg BW of furosemide, Dimazon®, Intervet, Beaucouzé, France) at the end of surgery and 3 mg/kg BW hydrochlorothiazide with 0.03 mg/kg BW dexamethasone (Diurizone®, Vétoquinol, Luré, France) for 2 days. One month after the surgery, a second scan session was performed; the sheep were again weighed, and blood samples were collected as described above to assess the efficiency of the surgery (Figs. 1A and S1).

2.3. Testosterone and progesterone assays

Plasma was obtained from heparinized blood after 30 min of centrifugation at 3500*g*. The concentration of testosterone was determined in duplicate samples using a radioimmunoassay as previously described (Hochereau-de Reviers et al., 1990). The sensitivity of this assay was 0.1 $ng.mL^{-1}$. The concentration of plasma progesterone was determined in duplicate samples using an immunoenzymatic assay as previously described (Chasles et al., 2016). The sensitivity of the progesterone assay was 0.25 $ng.mL^{-1}$ (Fig. 1A).

2.4. Anesthesia protocol

Before scanning, the sheep were first anesthetized by an intrajugular administration of a ketamine/xylazine mix (1 $mg.mL^{-1}$ ketamine/0.1 $mg.mL^{-1}$ xylazine, volume of injection 6.5 mL). After induction, the animal was intubated (8.5 mm probe, SON612, Centravet, France) and ventilated manually. The jugular vein was catheterized for a continuous infusion of 0.1 $mg.mL^{-1}$ ketamine/xylazine mix (1.5 $mL.min^{-1}$), which permits preservation of both pupillary and palpebral reflexes and of the regular spontaneous respiratory rate.

Since MRI investigation in animals requires that animals be sedated, we developed a specific protocol of anesthesia for both functional and morphometric acquisition. Indeed, functional connectivity is highly sensitive to the pharmacological class of anesthetics used, and numerous studies have demonstrated that the widely used isoflurane gas obscures the naturally occurring functional connectivity by inducing synchronous cortico-striatal fluctuations and silencing subcortical activity (Kalthoff et al., 2013; Liu et al., 2013; Paasonen et al., 2018). For this reason, we chose to use a low dose of ketamine/xylazine mix (Imalgene 500 mg/Rompun 2%, Centravet, France) for functional acquisitions and progressively replaced this with a standard isoflurane anesthesia for morphological acquisitions to reduce motion artifacts during long scanning.

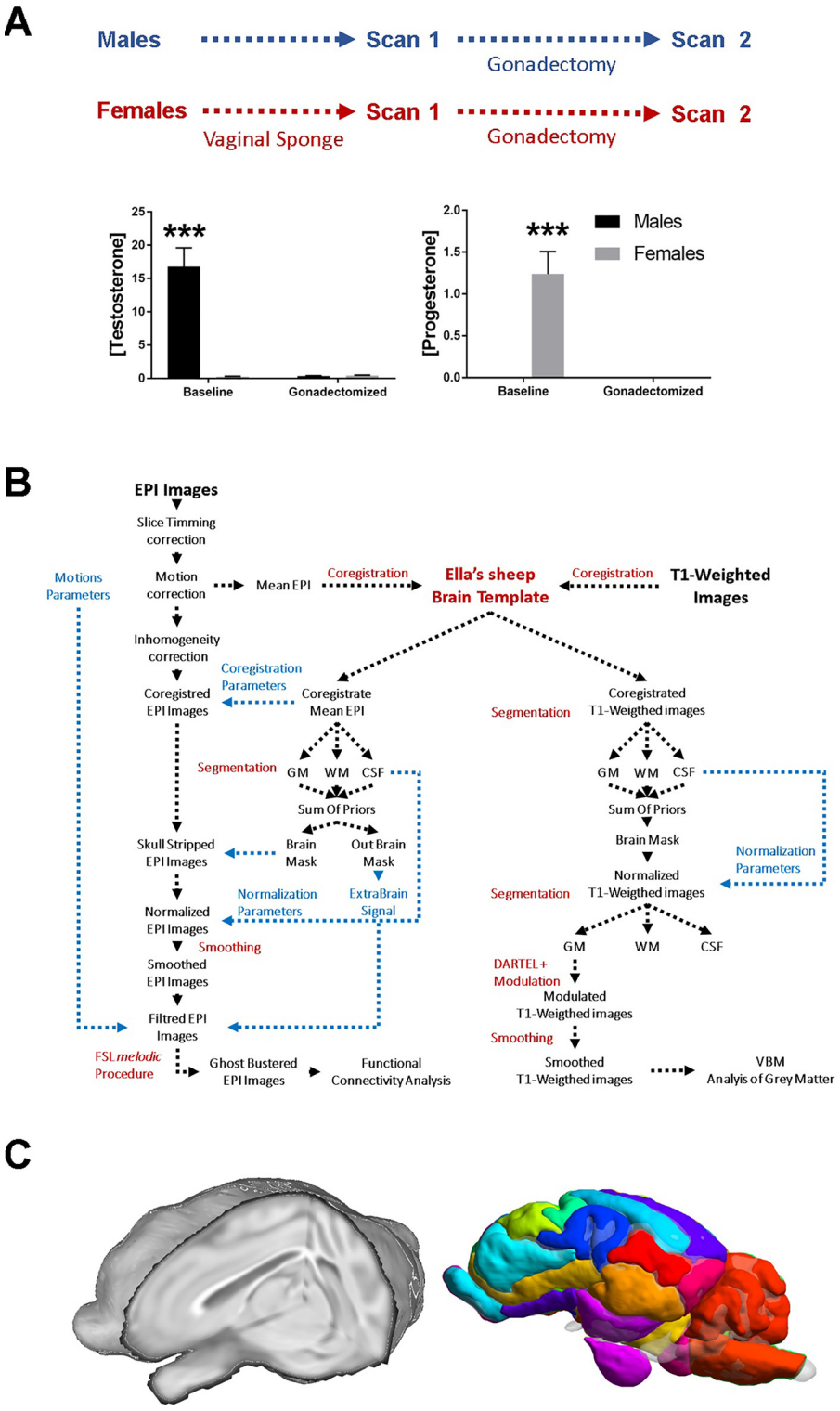

Fig. 1. Overview of the experiment. **A.** Experimental design and concentrations of testosterone and progesterone before and after gonadectomy in both males and females. **B.** Processing workflow for functional connectivity and voxel-based morphometry (VBM) analysis. Both functional and anatomical images are coregistrated onto the Ella' sheep brain template and then processed using a dedicated processing developed from SPM and FSL toolbox. **C.** 3D rendering of the Ella' sheep brain template and atlas. Sheep brain atlas is composed by a mosaic of 86 anatomical region of interest (ROI) which were used to create the functional connectivity matrix and functional networks analysis to identify brain territories revealed by the VBM analysis (for further information, see Material & Method section).
Data are compared using a two-way ANOVA followed by Holm-Sidak multiple comparisons test and expressed as mean ± SEM; *** $p < 0.001$.

2.5. Scanning procedure

Sheep were placed on the MRI-compatible mechanical bed of a 3 T VERIO Siemens system (Erlangen, Germany). They were gently restrained with a belt on the mechanical bed while their head was placed within a circular rigid coil (^{1}H, 24 channels, phased array, receiver only, 20/28 cm, P-H24LE-030, Siemens, Germany). During the functional resting state scanning procedure, sheep were ventilated continuously using an anesthesia system with an integrated ventilator (Aestiva MRI-compatible, GE Healthcare, Germany) delivering a 1:1 oxygen/air mix with a current volume of 500 ml for ewes and 650 ml for rams and the frequency rate set at 16 bpm. Heart rate and O_2 saturation were monitored continuously using an oximeter probe placed on the right hind paw (oxytip + probe MRI-compatible, GE Healthcare, Germany) and maintained at 87.21 ± 1.002 bpm and 89.83 ± 8.84% for ewes and 78.19 ± 9.28 bpm and 87.63 ± 6.18% for rams, respectively (for details see Fig. S1). After the functional resting state scanning procedure, the intravenous ketamine anesthesia regimen was progressively replaced by gas anesthesia using isoflurane added to the air mix at a concentration of 2.8 ± 0.14% in ewes and 3.07 ± 0.01%

in rams using the same ventilatory parameters (Fig. S1).

2.6. MRI data acquisition

Left-right orientation within the images was ensured by placing an α-tocopherol acetate capsule (Toco 500 mg, α-tocopherol acetate, Alkopharm, France) on the right side of the sheep's head. After positioning, a first localizer sequence was performed to align the brain on the anterior commissure-posterior commissure (AC-PC) axis within the field of view (FOV). Then, two successive gradient echoes (GRE) field maps were acquired using the same acquisition parameters: repetition time (TR) = 500 ms, echo time (TE) = 4.92 ms and 7.38 ms, number of excitations (NEX) = 1, flip angle (FA) = 55°, field of view = 166 × 166 × 166 mm^3 within a 64 × 64 × 64 matrix for a final voxel size = 2.6 × 2.6 × 2.6 mm^3. Both GRE field maps were acquired within the axial acquisition plane, but a left-right encoding direction was used on the first acquisition (LR-GRE); then, a right-left encoding direction was used on the second acquisition (RL-GRE). Both LR- and RL-GRE images were acquired to calculate inhomogeneity correction maps that were used within the functional analysis processing. Then, a spin-echo echo-planar imaging (SE-EPI) sequence of 8.5 min was acquired in the axial plane using the following parameters: TR = 3260 ms, TE = 24 ms, NEX = 1, FOV = 170 × 170 × 45 mm^3 within a 110 × 110 × 90 matrix for a final voxel size = 1.5 × 1.5 × 2 mm^3. This sequence generated 150 volumes that were used for resting-state fMRI analysis. Finally, a T1-weighted 3D magnetization-prepared rapid acquisition of gradient echo (MPRAGE) sequence was acquired using the following parameters: TR = 2500 ms, TE = 3.18 ms, FA = 12°, NEX = 2, FOV = 190 × 190 x 190 mm^3 within a 384 × 384 × 384 matrix for a final voxel size 0.5 × 0.5 × 0.5 mm^3. T1-weighted images were used for voxel-based morphometry analysis. Four rams were excluded from the analysis because of excessive motion during imaging acquisition, ($n_{(final)}$ = 8 males and 12 females). The final translations were less than 0.4 mm, and rotations did not exceed 0.006 radians (0.3 degrees) in our acquisitions (Fig. S2).

2.7. Functional MRI (fMRI) data preprocessing

Resting-state fMRI data were preprocessed in MATLAB (R2017b, MathWorks) with SPM8 (http://www.fil.ion.ucl.ac.uk/spm) using the SPMMouse Toolbox (Sawiak et al., 2014, 2009) and FSL5.1 (https://fsl.fmrib.ox.ac.uk). In the first step of preprocessing, the EPI images were time corrected, realigned and resliced to the first volume, corrected for inhomogeneity using the GRE field maps and coregistered with their corresponding T1 anatomical images using SPM8. Thereafter, T1 anatomical images were segmented using our previously published tissue priors (Ella et al., 2017), first to create specific brain masks for each T1 image (gray matter (GM) + white matter (WM) + cerebrospinal fluid (CSF) = Brain Mask) and second to normalize both T1 and EPI images onto our brain template (Ella et al., 2017) using the affine matrix calculated by SPM8 during the segmentation step. Finally, normalized images were masked to remove soft tissue using the brain masks generated previously and spatially smoothed with a Gaussian kernel of 8 mm full-width at half-maximum (FWHM). In the second step of preprocessing, EPI images were processed using FSL. The effect of the six previously calculated motion parameters, including translations and rotations and out brain signals, was removed from the data through linear regression using the FEAT toolbox (https://fsl.fmrib.ox.ac.uk/fsl/fslwiki/FEAT). Then, acquisition artifacts (ghosting) were identified using the *melodic* function. Briefly, *melodic* decomposes the signal of the 4D smoothed images into independent spatial components. These components were thresholded ($p < 0.01$) and visually inspected for artifacts, which were removed using the *regfilt* function of FSL (Kelly et al., 2010). Finally, a bandpass filtering (0.1 Hz-0.005 Hz) was applied to the time series (Fig. 1B).

2.8. Construction of resting-state functional networks

Pre- and post-gonadectomy, processed functional images of each animal (40 data sets) were segmented into 86 anatomical regions of interest (ROIs) (43 regions in each hemisphere) using the GM areas of our sheep atlas (Ella et al., 2017) and the REX function of the CONN toolbox (https://www.nitrc.org/projects/conn; Fig. 1B). For each sheep, functional correlation coefficients (r values) were computed between the time courses of each pair of ROIs and then transformed to z-scores using Fisher's z transformation, resulting in an 86 × 86 matrix of normalized correlation coefficients for each animal. Networks of altered connectivity were computed, extracted and plotted using Network-Based Statistics (NBS, http://brain-connectivity-toolbox.net/comparison/nbs; Zalesky et al., 2010), the Brain Connectivity Toolbox (http://brain-connectivity-toolbox.net; Rubinov and Sporns, 2010), the BrainNet Viewer toolbox (https://www.nitrc.org/projects/bnv/; Xia et al., 2013) and in-house developed MATLAB scripts. As the sample size was unbalanced between both sexes (8 males *versus* 12 females), we estimated the type 2 error (β value = 0.898) to assess the number of permutations necessary to reach a β value = 0.95 (n = 1500). Statistical comparisons between groups were made at the global network level (*i.e.*, conjunction of all ROIs). The NBS methodology works in two steps: first, the statistical hypothesis is tested at each connection, and its statistical significance is determined; second, the connections are thresholded by a user-defined significance ($p < 0.05$, < 0.01 and < 0.001); the subnetwork components (groups of nodes and edges such that a path can be found between any pair of network members) were found; and their size (number of surviving connections) was determined. The component significance was determined through permutation testing (n = 5000), where the test subjects are randomly permutated between groups and the chance of randomly finding networks of similar size determined, outputting a family-wise error rate-corrected significance (α_{FWE}, 0.05). Differences between gonad-intact males and females and the effect of gonadectomy on males and females were determined using analysis of variance (ANOVA) with group or time as a factor. A p value < 0.05 after correction was considered statistically significant. Considering the individual variability and as a control to test our statistical power, we compared two random groups balanced for sex (4 males and 6 females in each group; Fig. S3). At the baseline, male and female z scores described a Gaussian distribution ($K2_{(Males)}$ = 11.96; p = 0.0025 and $K2_{(Females)}$ = 13.93; p = 0.0009; D'Agostino & Pearson normality test) that was significantly different (p < 0.0001; t = 4.995; df = 354, paired *t*-test) with a shift of female values to the right. After gonadectomy, z scores also followed Gaussian distributions ($K2_{(Males)}$ = 20.41; p < 0.0001 and $K2_{(Females)}$ = 22.93; p < 0.0001) and were significantly different between the sexes (p < 0.0001; t = 9.848; df = 354), again with a shift of the female values to the right. When baseline z scores for males and females were mixed, the Gaussian distributions were conserved ($K2_{(Males)}$ = 14.77; p = 0.0006 and $K2_{(Females)}$ = 18.58; p < 0.0001), but the curves were superimposed and not significantly different (p = 0.4382; t = 0.7758; df = 708). The same effect was observed after gonadectomy ($K2_{(Males)}$ = 20.53; p < 0.0001 and $K2_{(Females)}$ = 21.5; p < 0.0001; z score comparison: p = 0.8802, t = 0.1507; df = 708).

2.9. Voxel-based morphometry (VBM) data preprocessing

VBM data were preprocessed with SPM8 and SPMMouse 1.1 Toolbox. First, each T1 anatomical image was aligned to the stereotaxic space by registering each image to our anatomical template image (Ella et al., 2017) using SPMMouse. Then, each image was bias corrected and segmented into probability maps of GM, WM, and CSF using the default settings in the SPM8 toolbox and our GM, WM, CSF probability maps (Ella et al., 2017). The transformation matrices obtained were used to normalize and resample (0.5 × 0.5 × 0.5 mm^3) the GM, WM and CSF

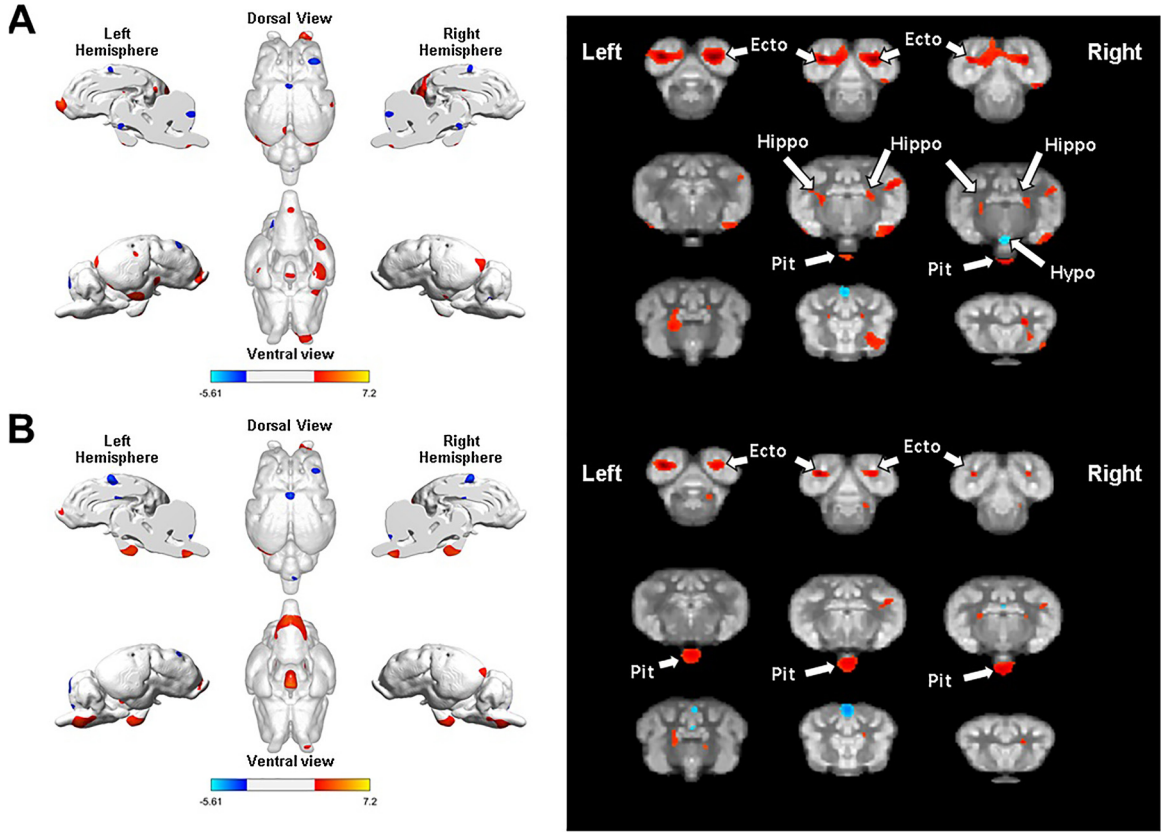

Fig. 2. Morphological brain sexual dimorphisms in intact and gonadectomized animals. Male *versus* female VBM comparison before and after the gonadectomy procedure. **A. left panel**: brain plots representing the surface map of regional grey matter concentration (GMC) differences between gonad-intact male *versus* luteal phase female sheep. **A. right panel**: brain slices showing GMC differences between intact male *versus* intact female sheep. **B. left panel**: brain plots representing the surface map of GMC differences between gonadectomized male *versus* gonadectomized female sheep. **B. right panel**: brain slices showing GMC differences between gonadectomized male *versus* gonadectomized female sheep.
Ecto = ectolateralis gyrus ; Hippo = hippocampus ; Pit = pituitary gland ; Hypo = hypothalamus. Data are the results of interaction analysis (**A**) males *versus*females at the baseline (**B**) males *versus* females after gonadectomy using a p value < 0.005 (β value = 0.990) corresponding to $t_{(35)} = 2.7238$ and a cluster threshold set at 300 voxels. N = 20 animals (8 males and 12 females).

probability maps. To produce a more accurate registration within each sheep as well as across all sheep, the Diffeomorphic Anatomical Registration Through Exponentiated Lie Algebra (DARTEL) algorithm, which is an automated, unbiased, and nonlinear template building program (Ashburner, 2007), was applied using the strategy described by (Asami et al., 2012). First, a subject-specific template was created by the DARTEL algorithm using the previous tissue class images (GM, WM, and CSF maps) obtained from each sheep at both time points (before and after gonadectomy). The DARTEL procedure releases individual-specific flow field maps, permitting the application of diffeomorphic normalization on each tissue class of images to spatially normalize each time point on a subject-specific template space. Each normalized tissue class of images was modulated by the determinant of the Jacobian to account for the expansion and/or contraction of brain regions over time. Then, a population-specific template was created by the DARTEL algorithm using all of the subject-specific templates of the tissue class of images. Here, the DARTEL procedure releases population-specific flow field maps, permitting the application of diffeomorphic normalization from each animal onto each tissue class of images. Finally, each tissue class image was modulated by the determinant of the Jacobian, and the final modulated GM images were spatially smoothed by convolving with a 4 mm full-width at half-maximum (FWHM) isotropic Gaussian kernel to create GMC maps (Fig. 1B) (Sumiyoshi et al., 2017).

2.10. Voxel-Based Morphometry, statistics and analysis

Statistical Parametric Mapping (SPM8) was used to reveal the temporal and regional changes in gray matter occurring in GMC maps. Second level analysis from SPM, a flexible factorial model that is equivalent to a 2 × 2 mixed-model ANOVA, was used first to compare male *versus* female and then pregonadectomy *versus* postgonadectomy groups. Brain volume was used as a covariate (Fig. S4A) with between-subject factor group and within-subject factor condition. The factors included in the analysis were subjects, group (male, female), and time (pregonadectomy, postgonadectomy). A brain mask was used to constrain the analysis. For each cluster, the significance of the peak voxel was set as $p <$ 0.005 (β value = 0.990, $t_{(35)} = 2.7238$), and the minimum cluster extent was set to 300 voxels. The results are presented on an axial brain slice series generated by the xjView plugin (http://www.alivelearn.net/xjview/) of SPM, and the corresponding surfacing results were assembled with a BrainNet viewer, which allows the generation of both brain mesh and brain plots for visualizing data. To assess the effect of individual variability and as a control test for statistical power, we compared two random groups balanced for sex (4 males and 6 females in each group (Fig. S4). At baseline, the comparison shows only a small significant unilateral cluster on slices 14 and 12 corresponding to the left lateral *gyrus,* which was not observed previously ($p =$ 0.005, β value = 0.990, $t_{(35)} = 2.7238$, voxel threshold = 300), while the comparison performed after the gonadectomy reveals no significant differences between the groups.

2.11. Postprocessing statistical analysis

VBM cluster peaks revealed by flexible factorial analysis data were

identified using our atlas and a personal procedure developed in MATLAB. For each comparison, ROI masks from Ella's atlas were used to extract GMC values of corresponding regions within the GMC map using REX plugging. Endocrine, physiological, functional connectivity and GMC data were compiled and analyzed using Prism 6.02 software GraphPad Software, San Diego, CA) and were compared using two-way ANOVA with repeated measures followed by the two-stage setup method of Benjamini, Kriegger and Yekutieli as recommended by the software. Statistical significance was defined as $p < 0.05$ for these analyses.

3. Results

3.1. Morphological and functional sexual dimorphism in the adult sheep brain

3.1.1. VBM analysis

Using a voxel-based morphometry (VBM) approach, we found 37 brain regions that were sexually dimorphic in intact sheep (see Tables S1 and S2 for detailed statistics). Specifically, our VBM analysis found that the gray matter concentration (GMC) within the left and right *gyrus ectolateralis*, left and right hippocampus, pituitary gland and right amygdala were significantly higher in intact females than in intact males (red clusters, Fig. 2A). In contrast, GMC values in the hypothalamus and both posterior gyri sigmoideus were significantly higher in intact males *versus* luteal phase females (blue clusters, Fig. 2A). Comparison between the same animals before and after gonadectomy reveals that only 22 brain regions were still dimorphic. Among them, four bilateral cortical regions of the gyri ectolateralis, both entolateral and lateral gyri, and the occipital lobe, still exhibited higher GMC values in gonadectomized females than in gonadectomized males (red clusters, Fig. 2B). GMC values in the posterior gyri sigmoideus were still higher in gonadectomized males than in gonadectomized females (blue, clusters, Fig. 2B). The volumes of several dimorphic subcortical structures, such as the right amygdala and the hypothalamus, decreased after gonadectomy and were no longer different between males and females. Moreover, we observed a large regression of the volume of the hippocampal cluster (120 mm^3 within the intact male/intact female comparison *versus* 15 mm^3 within the gonadectomized male/gonadectomized female comparison) and a large increase (10 times) of the volume of the pituitary cluster (28 mm^3 within the intact male/intact female comparison *versus* 280 mm^3 within the gonadectomized male/gonadectomized female comparison).

Using our anatomical atlas (Ella et al., 2017), we collected GMC values within the bilateral hippocampus, hypothalamus, pituitary gland and gyri ectolateralis to evaluate the effect of gonadectomy on these structures. Within the hippocampus (Fig. 3A), we observed a left-right asymmetry in both males and females as previously reported (Sadeghi et al., 2017; Samara et al., 2011), which was preserved after gonadectomy. In addition, we observed bilateral sexual dimorphism in the hippocampus with higher GMC values in luteal phase females than in intact males. This hippocampal sexual dimorphism was lost after gonadectomy. Within the hypothalamus (Fig. 3B), no left-right asymmetry was observed, but significantly higher GMC values were found in intact males compared to luteal phase females. The sexual dimorphism in the hypothalamus was also eliminated after gonadectomy. No side asymmetry was observed within the pituitary gland (Fig. 3C), but significantly higher GMC values were observed in luteal phase females compared to intact males. GMC concentration in the pituitary increased significantly in both sexes after gonadectomy, but sexual dimorphism was preserved. Finally, analysis of GMC within the gyri ectolateralis (Fig. 3D) revealed no left-right asymmetry, but GMC values were significantly higher in luteal phase females when compared to gonad-intact males.

3.1.2. Resting-state fMRI analysis

The analysis of the functional connectome between intact males and females revealed a sexually dimorphic brain network composed of 332 functional connections shared between 77 functional nodes (Fig. 4A, all statistics are available in Table S3). Intact luteal phase females displayed higher functional connectivity than intact males (Fig. 4B). Three internal subnetworks involving the frontal region (red nodes), the occipitoparietal region (orange nodes) and the diencephalic region (yellow nodes) compose this dimorphic network. When we focused on the sexually dimorphic brain regions highlighted by our previous VBM analysis, we observed that both the left and right hippocampus, hypothalamus pineal gland and gyrus ectolateralis display higher functional connectivity in luteal phase females when compared to intact males (Table S3). Notably, the hippocampus displayed stronger bilateral connections in luteal phase females than in intact males within the geniculate nucleus, the parahippocampal cortex, the periaqueductal gray substance (PAG), the suprasylvian *gyrus*, the cingulate cortex, the pineal gland, the temporal lobe and the thalamus. The hypothalamus displayed stronger bilateral connections in luteal phase females than in intact males within the lateral septal nucleus, the preoptic hypothalamic area, the subfornical organ and the substantia nigra. Importantly, the connectivity between the hypothalamus and the pituitary gland was also significantly higher in luteal phase females than in intact males. Finally, the gyrus ectolateralis displayed stronger bilateral connections in luteal phase females than in intact males within the gyri entolateralis and the lateral gyri.

Surprisingly, the analysis of the functional connectome between gonadectomized males and females revealed a similar brain network also composed of 332 functional connections shared between 80 functional nodes (Fig. 4C, all statistics are available in Table S4). This functional network is characterized by higher functional connectivity in gonadectomized females when compared to gonadectomized males (Fig. 4D) and displayed the same internal frontal, occipitoparietal and diencephalic subnetworks. Although it was statistically marginal, some changes in resting-state functional connectivity were also detected within the hippocampus, hypothalamus, and gyrus ectolateralis. Similar temporal correlations were observed within the previously described structures. Additional bilateral connections were observed within the gyrus ectolateralis, midbrain, left lateral *gyrus* and right nucleus of the horizontal limb of the diagonal band (NHLDB) of gonadectomized females compared to gonadectomized males. Within the hypothalamus, similar functional connectivity was observed to that described in intact animals. Additional functional connectivity was observed with the lateral septal nucleus bilaterally in gonadectomized females when compared to gonadectomized males and with the right bed nucleus of the stria terminalis (BNST), the left globus pallidum and the left NHLDB. Finally, the gyrus ectolateralis also displayed similar higher functional connections with previously described structures and additional bilateral functional connectivity with the cingulate cortex, the occipital lobe, the suprasylvian gyrus and the hippocampus. Functional connections were also observed with the right parahippocampal cortex, the right posterior sylvian *gyrus* and the right temporal lobe in gonadectomized females when compared to gonadectomized males.

3.2. Effect of gonadal secretion on brain morphology and functional connectivity in both male and female adult sheep brains

3.2.1. VBM analysis

To evaluate the sex-specific effects of gonadectomy, we evaluated both brain morphology and functional connectome modifications before and after gonadectomy in males and females. In males, VBM analysis revealed 29 regions with significant GMC modifications induced by gonadectomy (see Table S5 for detailed statistics). We found significantly higher GMC values within the bilateral amygdala and the pituitary gland after gonadectomy (red clusters, Fig. 5A). On the other hand, the GMC values were significantly decreased after gonadectomy

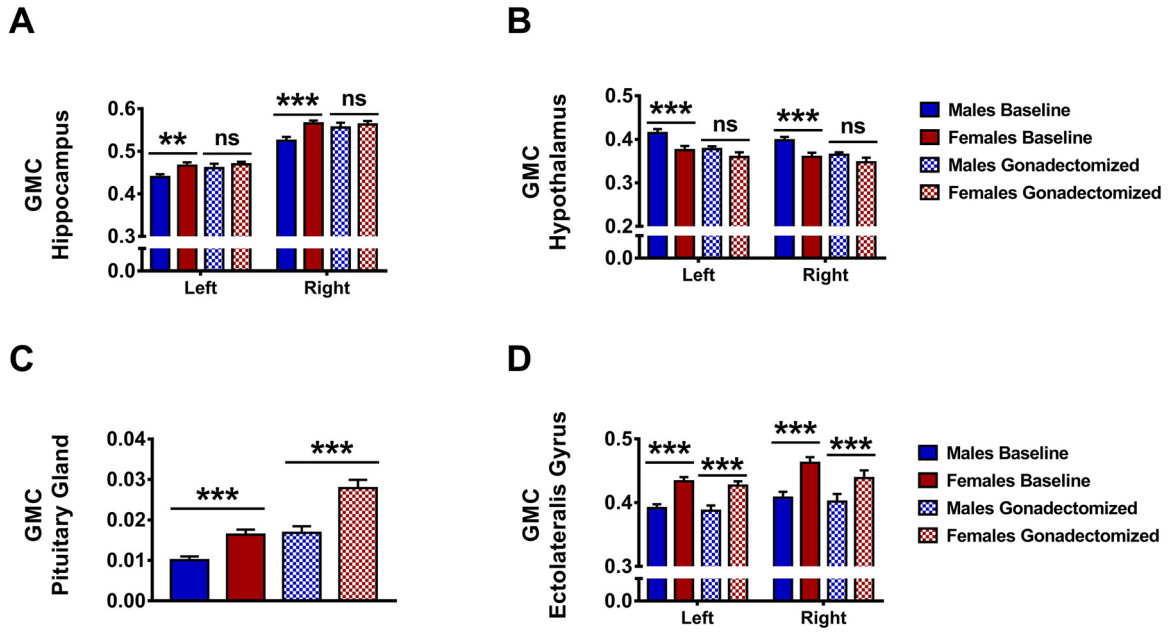

Fig. 3. Effect of gonadectomy on sexually dimorphic structures. The mean values of Grey Matter Concentration (GMC) were evaluated bilaterally in **A.** hippocampus, **B.** hypothalamus, **C.** pituitary gland and **D.** ectolateralis gyrus for both male and female sheep before and after gonadectomy.
Data were compared using a two-way ANOVA followed by Holm-Sidak multiple comparisons test and expressed as mean ± SEM; *$p < 0.05$; ** $p < 0.01$ and *** $p < 0.001$. N = 20 animals (8 males and 12 females).

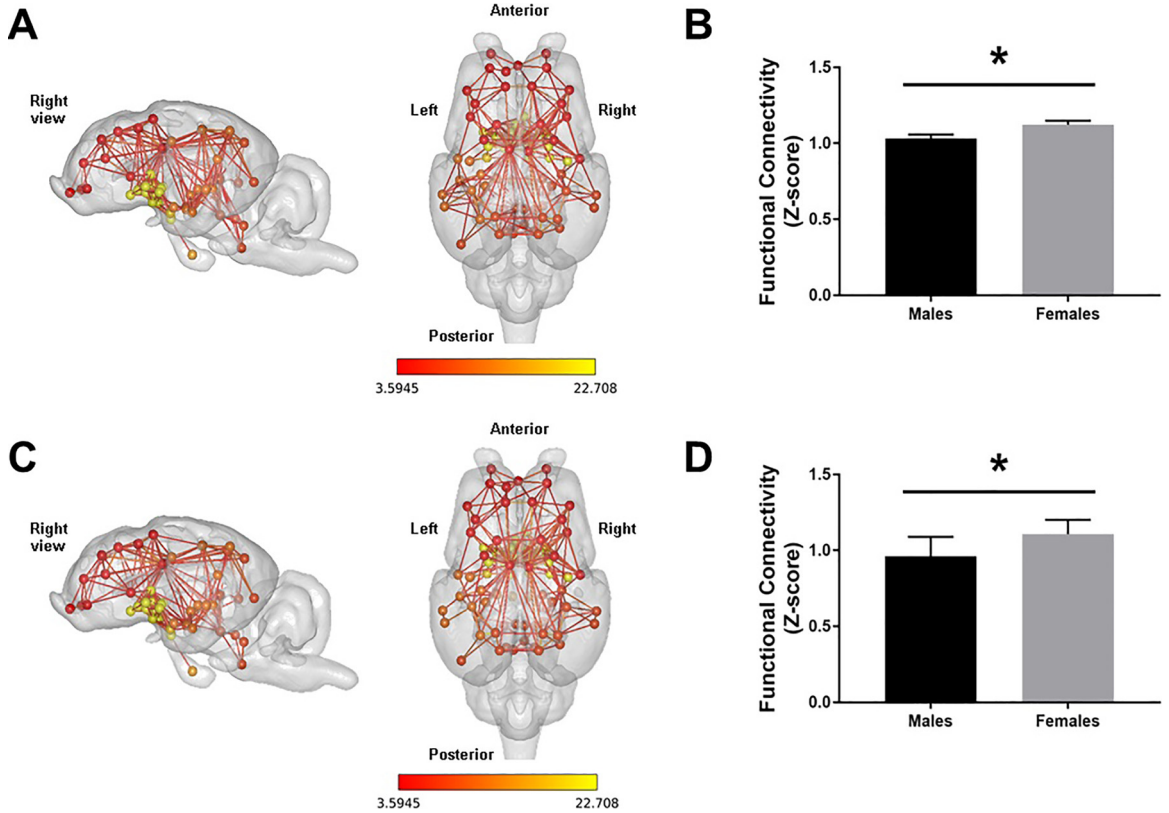

Fig. 4. Functional brain sexual dimorphisms in intact and gonadectomized sheep. **A.** Sagittal and dorsal view of the sexually dimorphic brain functional network between entire males *versus* entire females. **B.** Mean connectivity values within the previous network between entire males and entire females. **C.** sagittal and dorsal view of the sexually dimorphic brain functional network between gonadectomized males *versus* gonadectomized females. **D.** Mean connectivity values within the previous network between gonadectomized males and gonadectomized females.
The sexually dimorphic functional network are the results of interaction analysis between (**A**) males *versus* females at the baseline and between (**C**) males *versus* females after gonadectomy using network-based statistics (NBS; connection-level threshold *p*-uncorrected < 0.001, networks were significant at $p < 0.05$ family-wise error (FWE) corrected), nodes and edges colour coded according to statistical strength (*t*-value). Both comparison of the mean values of the networks were evaluated using a two-tailed Student *t*-test and expressed as mean ± SEM; *$p < 0.05$. N = 20 animals (8 males and 12 females).

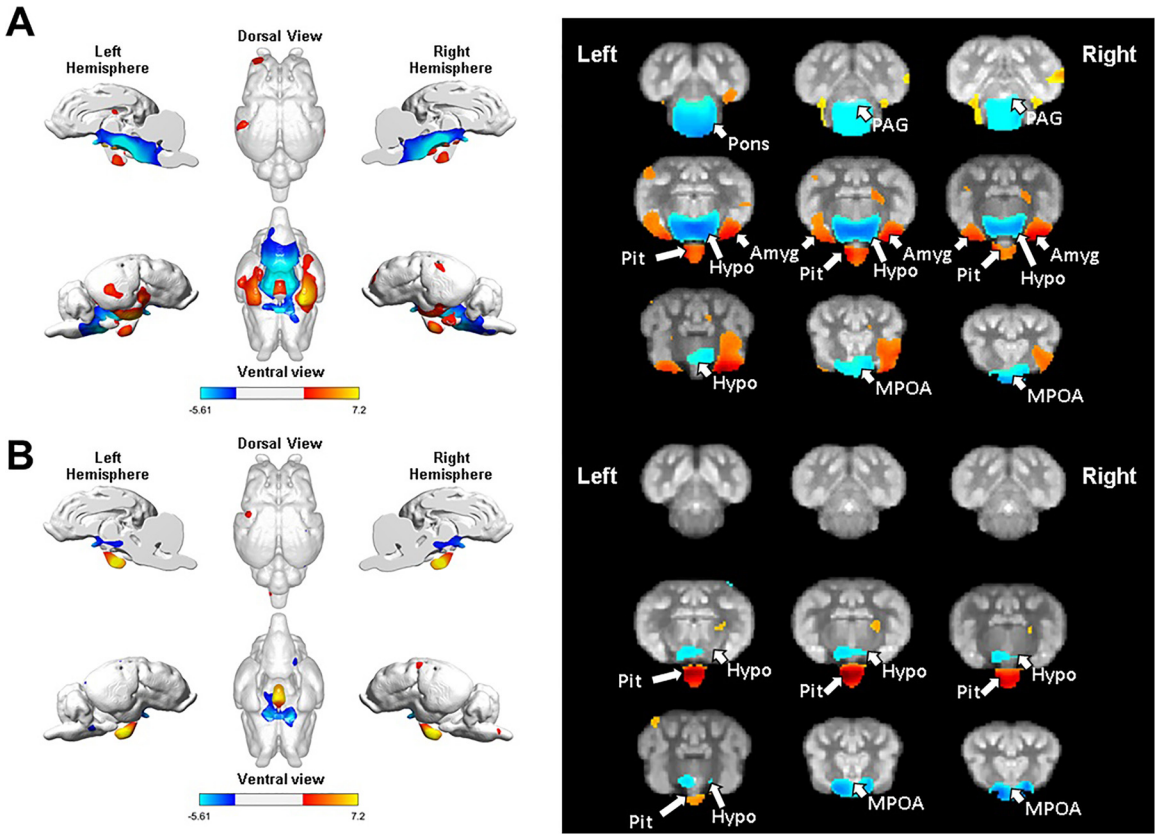

Fig. 5. Effect of the gonadectomy procedure in both males and females on brain morphology. **A. left panel**: brain plots representing the surface map of regional grey matter concentration (GMC) differences between entire male *versus* gonadectomized male. **A. right panel**: brain slices showing GMC differences between entire male *versus* gonadectomized male. **B. left panel**: brain plots representing the surface map of GMC differences between entire female *versus* gonadectomized female. **B. right panel:** brain slices showing GMC differences between entire female *versus* gonadectomized female.
PAG : periaqueductal grey ; Amyg = amygdala ; Pit = pituitary gland; Hypo = hypothalamus ; MPOA = medial preoptic area. Data are the results of interaction analysis between (**A**) baseline *versus* gonadectomy in males and between (**B**) baseline *versus*gonnadectomy in female using a p value < 0.005 (β value = 0.990) corresponding to $t_{(35)}$ = 2.7238 and a cluster threshold set at 300 voxels. N = 8 in male group and n = 12 in female group.

within the medial mamillary nucleus, the periaqueductal gray substance (PAG), the pons and the medial preoptic hypothalamic area (blue clusters, Fig. 5A). In females, VBM analysis revealed 22 regions with significant GMC modifications induced by gonadectomy (see Table S6 for detailed statistics). We found significantly higher GMC values only within the pituitary gland (red clusters, Fig. 5B). By contrast, GMC values were significantly decreased within the medial mamillary nucleus, *medulla oblongata* (MO), pons and preoptic hypothalamic area (blue clusters, Fig. 5B). Interestingly, after gonadectomy, GMC values were also reduced within both gyri ectolateralis but only within the right hemisphere (Fig. 5B).

Using our anatomical atlas, we collected GMC values within the bilateral amygdala and PAG in males and within the subfornical organ and NHLDB in females, which display sex-specific modifications after gonadectomy. In males, GMC was significantly increased after gonadectomy within the amygdala (Fig. 6A left panel). On the other hand, the GMC values within the PAG were significantly decreased after gonadectomy (Fig. 6A, right panel). In females, GMC values were significantly decreased after gonadectomy within the subfornical organ (Fig. 6B left panel). GMC values within the NHLDB were also significantly decreased after gonadectomy (Fig. 6B, right panel).

3.2.2. Resting-state fMRI analysis

The analysis of the functional connectome between intact and gonadectomized males revealed a brain network sensitive to gonadal hormones composed of 66 functional connections shared between 52 functional nodes (Fig. 7A, all statistics are available in Table S7). This functional network was significantly higher in gonadectomized males (Fig. 7A, Right panel) and was characterized by modifications of rostrocaudal functional connectivity and by intense modifications of functional connectivity within the diencephalon. Importantly, the pituitary gland, which is a critical structure in reproductive function and shows significant variations of GMC after gonadectomy, displayed increased functional connectivity together with the preoptic hypothalamic area, the BNST and the subfornical organ. By contrast, the analysis of the functional connectome between intact and gonadectomized females revealed a brain network sensitive to gonadal hormones composed of 94 functional connections shared between 65 functional nodes (Fig. 7B, all statistics are available in Table S8). This functional network was also significantly higher in gonadectomized females (Fig. 7B, Right panel) and was characterized by an interhemispheric modification of functional connectivity and, as previously described in males, by intense modifications of functional connectivity within the diencephalon. As observed in males, the pituitary gland also displayed an increase in GMC after gonadectomy in females along with an increase in the functional connectivity within the medial septal nucleus, the BNST, the septum, the NHLBD, the preoptic hypothalamic area and the subfornical organ.

4. Discussion

Our study is the first to report a detailed VBM analysis in sheep and to establish resting-state fMRI in this species. Thanks to these methodological developments, we were able to highlight brain sexual dimorphic territories and networks of functional connectivity differing between males and females, mainly in the hypothalamus and pituitary.

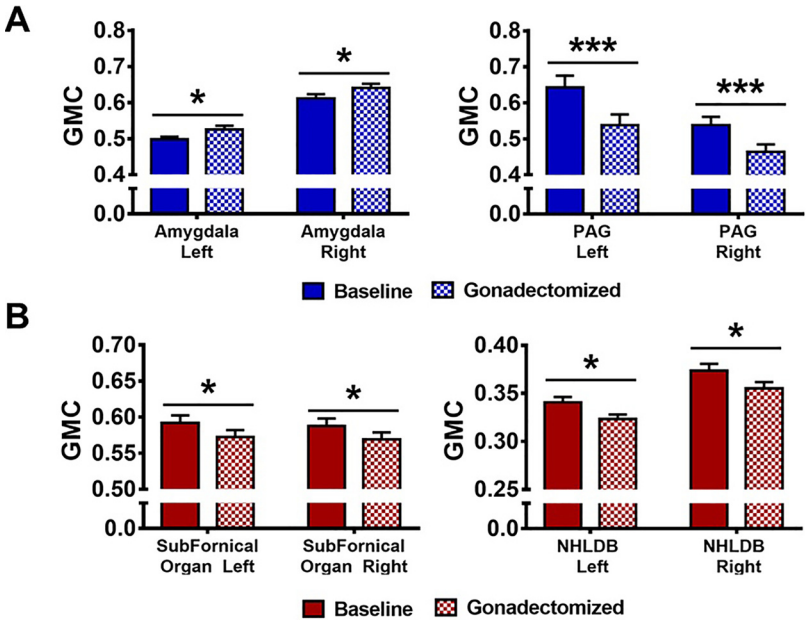

Fig. 6. Effect of the gonadectomy procedure on non-sexually dimorphic structures in both male and female sheep. In males, the mean grey matter concentration (GMC) values were evaluated bilaterally within **A.** the amygdala (Left), and the periaqueductal grey substance (PAG, Right). In females, the mean GMC values were evaluated bilaterally within **B.** the subfornical organ (Left), and the nucleus of the horizontal limb of the diagonal band (NHLDB, Right).
Data were compared using a two-way ANOVA followed by Holm-Sidak multiple comparisons test and expressed as mean ± SEM; *$p < 0.05$ and *** $p < 0.001$. N = 8 in male group and n = 12 in female group.

We also showed that these differences are partly due to adult circulating levels of gonadal hormones, as some of these differences vanished following gonadectomy, suggesting that the differences observed are due to the activational effects of circulating gonadal hormones. These data add a high degree of neuroanatomical precision compared to the previous MRI report of differences between the sexes in sheep (Nuruddin et al., 2013) and were made possible through the construction of an adapted brain template and atlas of the ovine brain (Ella et al., 2017;

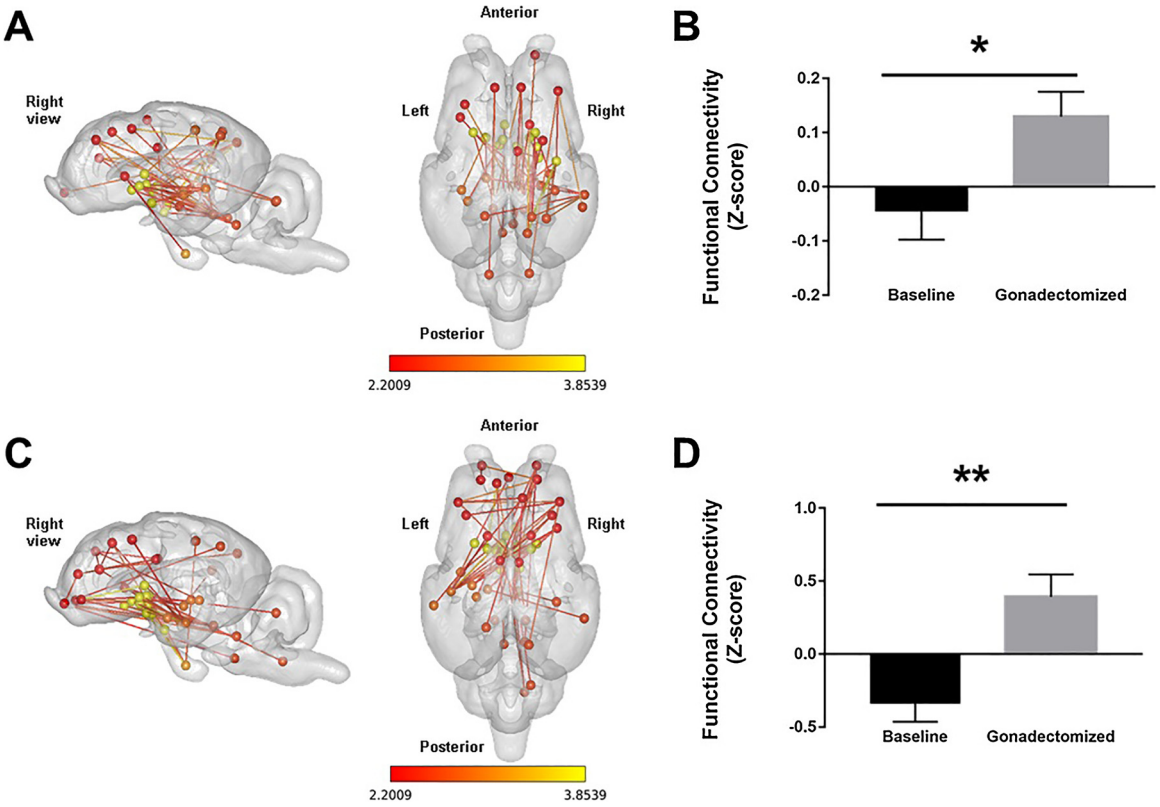

Fig. 7. Effect of the gonadectomy procedure on brain functional connectivity in male and female sheep. **A.** Sagittal and dorsal view of the altered functional network induced by gonadectomy in males. **B.** Mean connectivity values within the previous network between entire *versus* gonadectomized males. **C.** Sagittal and dorsal view of the altered functional network induced by gonadectomy in females **D.** right panel: Mean connectivity values within the previous network between gonad-intact or luteal phase females *versus*gonadectomized females.
The sexually dimorphic functional network are the results of interaction analysis between (**A**) baseline *versus* gonadectomy in male group and between (**B**) Baseline *versus*gonadectomy in female group using network-based statistics (NBS; connection-level threshold *p*-uncorrected < 0.05, networks were significant at $p < 0.05$ family-wise error (FWE) corrected), nodes and edges colour coded according to statistical strength (*t*-value). Both comparison of the mean values of the networks were evaluated using a two-tailed Student *t*-test and expressed as mean ± SEM; *$p < 0.05$ and ** $p < 0.01$. N = 8 in male group and n = 12 in female group.

Ella and Keller, 2015).

4.1. Sex differences in intact animals

4.1.1. VBM analysis

First, our VBM analysis revealed clear differences in GMC between intact males and females in five main areas: the hippocampus, the hypothalamus—especially the arcuate region—the pituitary, the amygdala and the gyrus ectolateralis. For all these regions, with the exception of the hypothalamus, GMC was higher in males than in females. On the whole, the differences measured in the hypothalamus and pituitary, which are key components of the gonadotropic axis, are not very surprising because the axis is known to be highly sexually dimorphic. Indeed, sexual differences have been previously reported in other species or by other approaches in these areas. For example, similar to our results, MRI studies in humans have reported that the volume of the hypothalamus is larger in men than women (Goldstein et al., 2001; Makris et al., 2013). The hypothalamic cluster differing significantly between males and females appears to include the region of the arcuate nucleus, a structure where the numbers of neurons expressing kisspeptin, neurokinin B and dynorphin (KNDy neurons) as well as progesterone receptors are higher in female than in male sheep (Cheng et al., 2010). This difference is linked to the fact that KNDy neurons mediate the negative feedback of progesterone on GnRH secretion in females. In the hypothalamic cluster, other regions, such as the ventromedial nucleus, are also known to be sexually dimorphic, being larger in males than females (Flanagan-Cato, 2011). Finally, it is important to note that a limitation of our study is the level of resolution that is achievable using our MRI conditions (500 µm isovoxel resolution). This level of resolution prevents visualization of very small neuron clusters, such as the sexually dimorphic nucleus of the medial preoptic area, which has been consistently shown to be larger in males than females, including in sheep (Roselli and Stormshak, 2010). In the pituitary, we found that females have a higher concentration of gray matter than males. A recent human MRI study demonstrated that the pituitary fossa, which grossly reflects the volume of the pituitary, is larger in women than men (Pecina et al., 2017), thus corroborating our observations.

In the amygdala, we confirmed the sexual dimorphism previously reported in sheep (Nuruddin et al., 2013) and recently in humans (Lotze et al., 2019). At the cellular level, it has been shown that the size of neurons in the amygdala, as well as the content in estradiol receptors, is higher in male than female sheep (Alexander et al., 2001; Perkins et al., 1995). In other animal models, for example, in the rat, the volume of the medial amygdala is also higher in males than females (Cooke et al., 1999). The hippocampus is another brain region that appears to be sexually dimorphic in our study. As the hippocampus is a primary site for the regulation of cognitive processes such as stress responses or spatial memory, which are also influenced by gonadal hormones, such a difference is not surprising (Juraska, 1991; McCarthy and Konkle, 2005). In addition, our results showing that part of the anterior hippocampus is larger in females than males is congruent with a recent MRI study in mice (Meyer et al., 2017). Finally, the difference measured in the gyrus ectolateralis is more surprising because it is not known as a traditional region related to sex differences. Given the lack of anatomical and functional data regarding this region in sheep, it is difficult to interpret this result. It has been shown that the gyrus ectolateralis is part of the visual cortex (Clarke and Whitteridge, 1976), but further studies will be needed to assess the nature and role of this dimorphism.

We performed the same VBM comparison one month following gonadectomy to assess whether the differences observed are due to adult circulating levels of gonadal hormones. It is striking to note that most of the observed differences diminished significantly after gonadectomy, particularly in the hypothalamus and amygdala. Interestingly, adult castration of male rats induces a reduction of the volume of the medial amygdala to a level comparable to that observed in females, demonstrating that adult hormone manipulation can completely reverse the sexual dimorphism observed in intact animals. Interestingly, this region is also rich in aromatase and steroid receptors in adult sheep (Lehman et al., 1993; Roselli et al., 1998).

4.1.2. Resting-state fMRI

In addition to VBM analysis, our study is the first to report that the resting state connectome differs between male and female sheep. This analysis revealed a sexually dimorphic brain network composed of 332 functional connections shared between 77 functional nodes that displays increased functional connectivity in intact luteal phase females when compared to intact males. Three internal subnetworks involving the frontal region, the occipitoparietal region and the diencephalic region compose this dimorphic network, with the diencephalic region being by far the most sexually dimorphic. Interestingly, the functional connectivity within the diencephalic region and especially in the hypothalamic regions showed the highest degree of sexual dimorphism. Finally, these sexual differences were not significantly influenced by adult circulating gonadal hormones, as the network differing between the sexes was not influenced by gonadectomy.

4.2. Sex differences in gonadectomized animals

4.2.1. VBM analysis

When considering the effect of gonadectomy within each sex in the VBM analysis, it is striking to observe that gonadectomy induced very similar changes in GMC at the level of the hypothalamus and pituitary in both males and females. The fact that gonadectomy abolishes negative feedback (of testosterone for the males and progesterone for the females) is in line with a similar response of the hypothalamic-pituitary axis in both sexes. However, it is notable that in terms of GMC variations, the responses of the hypothalamus and pituitary were opposite. While an increase of GMC was observed in the pituitary following gonadectomy, a clear reduction was measured in the whole hypothalamus. The increase in GMC observed in the pituitary is in line with previous data showing that ovariectomy induces a strong increase in the number and size (2- to 3-fold hypertrophy) of the LH cell population in ewes (Polkowska et al., 1980).

By contrast, the medial preoptic area of the hypothalamus is long known to be highly sexually dimorphic in many species, including humans (Swaab et al., 1992). The size of the ovine sexually dimorphic nucleus, measured either by Nissl staining or the expression of aromatase, is significantly larger in adult rams than in ewes and is not affected by gonadectomy (Roselli et al., 2004, 2000). In contrast, gonadectomy induced a significant reduction in GMC in the hypothalamus in both sexes. This pattern of response remains to be explained in terms of cellular mechanisms.

4.2.2. Resting-state fMRI

When analyzing the effect of gonadectomy within each sex for resting-state fMRI, it is striking to first notice that within each sex, gonadectomy induced an increase in functional connectivity. The pituitary gland, which displayed an increase in GMC after gonadectomy, also expressed an increase in functional connectivity within the preoptic hypothalamic area and the BNST. However, intense modifications of functional connectivity within the diencephalon diverged according to sex. Indeed, while changes in males were characterized by rostrocaudal modifications of functional connectivity, changes were mostly interhemisphepric in females. The meaning of such differences remains to be explored in the future.

4.3. General considerations

As already mentioned, differences between sexes or between intact and gonadectomized animals are mainly located at the level of the hypothalamus and pituitary, reflecting differences in the regulation of

the gonadotropic axis. To fully validate the role of adult circulating sex steroids, especially testosterone and progesterone, in the maintenance of these sexual differences and determine which of these hormones is involved, it will be necessary in a future study to supplement gonadectomized animals with adult levels of circulating steroids and see whether we are able to restore the initial pattern of differences observed in intact animals.

Finally, it is important to consider several limitations that arise from the segmentation of our brain atlas and the use of anesthetics in preclinical fMRI investigation. First, the current level of anatomical/functional mapping of sheep brain neuroanatomy is far less precise than those in other species such as rodents. Even if more than 80 brain structures have been segmented so far, it should be remembered that MRI segmentation is dependent upon the contrasts on MRI images that can differ from histological observations. Consequently, each label includes many brain structures, and thus labeling would differ from the expectation of the reader. Second, in our analysis, we failed to find any functional connectivity that was higher in males than in females. Indeed, sex differences in ketamine sensitivity have been reported to affect the depth, duration and efficacy of anesthesia (Molina et al., 2016). Thus, even though measures of heart rate and O_2 saturation during functional acquisitions are similar between sexes (Fig. S1), a differential effect of ketamine on the resting-state network cannot be excluded. Moreover, the greater sensitivity to ketamine displayed by males could obscure differences physiologically present in males rather than in females, explaining the lack of higher functional connectivity in males compared to females. Finally, our analysis was performed using Ella's Sheep brain template and its associated probabilistic tissue maps, which were created from 18 ewes. Recent studies have proposed using a more specific template to improve the segmentation step (Fillmore et al., 2015; Huang et al., 2010). Hence, the development of a mixed brain template (including males and females) with a higher number of animals (n = 100, sex ratio 1:1) will be mandatory to improve the segmentation step and further develop future MRI studies using sheep.

In conclusion, we demonstrated that MRI is a suitable method to study neuroendocrine mechanisms that sustain sexual differences in the sheep brain and by inference in other large animal models. In this context, sheep offer a unique mammalian model in which to study neuroendocrine sexual differentiation and same-sex sexual partner preferences. Indeed, males showing spontaneous preference for other rams (male-oriented) represent as many as 8% of the ram population (Roselli et al., 2011; Roselli and Stormshak, 2009a, 2010). The understanding of the biological determinants and underlying neural networks mediating sexual attraction and mate selection are still quite incomplete in these animals. Thus far, evidence supports the idea of an organization of neural substrates by testosterone during prenatal development (Roselli and Stormshak, 2009a,b). While much attention has been given to the sexually dimorphic nucleus of the hypothalamus, a structure that cannot be observed in MRI due to the limits of resolution, MRI could provide new insights on whether the anatomy of other brain structures differ in male-oriented sheep.

Declaration of Competing Interest

The authors state that they have no conflict of interest.

Acknowledgments

We thank Didier Chesneau and Chantal Porte for their valuable help at different stages of this project. We thank all the shepherds, especially Damien Capo, Olivier Lasserre and Didier Dubreuil, from the experimental unit (UEPAO) for the care provided to the animals. We are also grateful to Anne-Lyse Lainé, Corinne Laclie and Dominique Gennetay from the laboratoire de Phénotypage-Endocrinologie for hormonal assays. We thank all the staff from the CIRE platform for their help during surgeries and imaging sessions, especially Gilles Gomot, Christian Moussu and Frédéric Elleboudt. Finally, we thank Julie Bakker, Charlotte Cornil and Jacques Balthazart for helpful feedback on this manuscript. This project was funded by grants from the French Agence Nationale de la Recherche (ANR) and the regional council Centre-Val-de-Loire (Pherobouc project). Additional funding to CER provided by NIH R01 OD011047.

Appendix A. Supplementary data

Supplementary material related to this article can be found, in the online version, at doi:https://doi.org/10.1016/j.psyneuen.2019.104387.

References

Alexander, B.M., Rose, J.D., Stellflug, J.N., Fitzgerald, J.A., Moss, G.E., 2001. Low-sexually performing rams but not male-oriented rams can be discriminated by cell size in the amygdala and preoptic area: a morphometric study. Behav. Brain Res. 119, 15–21. https://doi.org/10.1016/S0166-4328(00)00335-1.

Alexander, B.M., Skinner, D.C., Roselli, C.E., 2011. Wired on steroids: sexual differentiation of the brain and its role in the expression of sexual partner preferences. Front. Endocrinol. 2, 42. https://doi.org/10.3389/fendo.2011.00042.

Arnold, A.P., 2009. The organizational-activational hypothesis as the foundation for a unified theory of sexual differentiation of all mammalian tissues. Horm. Behav. 55, 570–578. https://doi.org/10.1016/j.yhbeh.2009.03.011.

Asami, T., Bouix, S., Whitford, T.J., Shenton, M.E., Salisbury, D.F., McCarley, R.W., 2012. Longitudinal loss of gray matter volume in patients with first-episode schizophrenia: DARTEL automated analysis and ROI validation. NeuroImage 59, 986–996. https://doi.org/10.1016/j.neuroimage.2011.08.066.

Ashburner, J., 2007. A fast diffeomorphic image registration algorithm. NeuroImage 38, 95–113. https://doi.org/10.1016/j.neuroimage.2007.07.007.

Bakker, J., Baum, M.J., 2008. Role for estradiol in female-typical brain and behavioral sexual differentiation. Front. Neuroendocrinol. 29, 1–16. https://doi.org/10.1016/j.yfrne.2007.06.001.

Burke, S.M., Kreukels, B.P.C., Cohen-Kettenis, P.T., Veltman, D.J., Klink, D.T., Bakker, J., 2016. Male-typical visuospatial functioning in gynephilic girls with gender dysphoria - organizational and activational effects of testosterone. J. Psychiatry Neurosci. JPN 41, 395–404. https://doi.org/10.1503/jpn.150147.

Burke, S.M., Veltman, D.J., Gerber, J., Hummel, T., Bakker, J., 2012. Heterosexual men and women both show a hypothalamic response to the chemo-signal androstadienone. PLoS One 7, e40993. https://doi.org/10.1371/journal.pone.0040993.

Chasles, M., Chesneau, D., Moussu, C., Delgadillo, J.A., Chemineau, P., Keller, M., 2016. Sexually active bucks are efficient to stimulate female ovulatory activity during the anestrous season also under temperate latitudes. Anim. Reprod. Sci. 168, 86–91. https://doi.org/10.1016/j.anireprosci.2016.02.030.

Cheng, G., Coolen, L.M., Padmanabhan, V., Goodman, R.L., Lehman, M.N., 2010. The kisspeptin/neurokinin B/dynorphin (KNDy) cell population of the arcuate nucleus: sex differences and effects of prenatal testosterone in sheep. Endocrinology 151, 301–311. https://doi.org/10.1210/en.2009-0541.

Clarke, I.J., Cummins, J.T., 1982. The temporal relationship between gonadotropin releasing hormone (GnRH) and luteinizing hormone (LH) secretion in ovariectomized ewes. Endocrinology 111, 1737–1739. https://doi.org/10.1210/endo-111-5-1737.

Clarke, P.G., Whitteridge, D., 1976. The cortical visual areas of the sheep. J. Physiol. 256, 497–508. https://doi.org/10.1130/jphysiol.1976.sp011335.

Cooke, B.M., Tabibnia, G., Breedlove, S.M., 1999. A brain sexual dimorphism controlled by adult circulating androgens. Proc. Natl. Acad. Sci. U. S. A. 96, 7538–7540 101073/pnas.96.13.7538.

Ella, A., Delgadillo, J.A., Chemineau, P., Keller, M., 2017. Computation of a high-resolution MRI 3D stereotaxic atlas of the sheep brain. J. Comp. Neurol. 525, 676–692. https://doi.org/10.1002/cne.24079.

Ella, A., Keller, M., 2015. Construction of an MRI 3D high resolution sheep brain template. Magn. Reson. Imaging 33, 1329–1337. https://doi.org/10.1016/j.mri.2015.09.001.

Fillmore, P.T., Phillips-Meek, M.C., Richards, J.E., 2015. Age-specific MRI brain and head templates for healthy adults from 20 through 89 years of age. Front. Aging Neurosci. 7. https://doi.org/10.3389/fnagi.2015.00044.

Flanagan-Cato, 2011. Sex differences in the neural circuit that mediates female sexual receptivity. Front. Neuroendocrinol. 32, 124–136. https://doi.org/10.1016/j.yfrne.2011.02.008.

Foster, D.L., Padmanabhan, V., Wood, R.I., Robinson, J.E., 2002. Sexual differentiation of the neuroendocrine control of gonadotrophin secretion: concepts derived from sheep models. Reprod. Camb. Engl. Suppl. 59, 83–99.

Goldstein, J.M., Seidman, L.J., Horton, N.J., Makris, N., Kennedy, D.N., Caviness, V.S., Faraone, S.V., Tsuang, M.T., 2001. Normal sexual dimorphism of the adult human brain assessed by in vivo magnetic resonance imaging. Cereb. Cortex N. Y. N 1991 11, 490–497. https://doi.org/10.1093/cercor/11.6.490.

Hochereau-de Reviers, M.T., Perreau, C., Pisselet, C., Fontaine, I., Monet-Kuntz, C., 1990. Comparisons of endocrinological and testis parameters in 18-month-old Ile de France and Romanov rams. Domest. Anim. Endocrinol. 7, 63–73. https://doi.org/10.1016/0739-7240(90)90055-5.

Huang, C.-M., Lee, S.-H., Hsiao, I.-T., Kuan, W.-C., Wai, Y.-Y., Ko, H.-J., Wan, Y.-L., Hsu,

Y.-Y., Liu, H.-L., 2010. Study-specific EPI template improves group analysis in functional MRI of young and older adults. J. Neurosci. Methods 189, 257–266. https://doi.org/10.1016/j.jneumeth.2010.03.021.
Juraska, J.M., 1991. Sex differences in "cognitive" regions of the rat brain. Psychoneuroendocrinology 16, 105–109. https://doi.org/10.1016/0306-4530(91)90073-3.
Kalthoff, D., Po, C., Wiedermann, D., Hoehn, M., 2013. Reliability and spatial specificity of rat brain sensorimotor functional connectivity networks are superior under sedation compared with general anesthesia. NMR Biomed. 26, 638–650. https://doi.org/10.1002/nbm.2908.
Kelly, R.E., Alexopoulos, G.S., Wang, Z., Gunning, F.M., Murphy, C.F., Morimoto, S.S., Kanellopoulos, D., Jia, Z., Lim, K.O., Hoptman, M.J., 2010. Visual inspection of independent components: defining a procedure for artifact removal from fMRI data. J. Neurosci. Methods 189, 233–245. https://doi.org/10.1016/j.jneumeth.2010.03.028.
Lehman, M.N., Ebling, F.J., Moenter, S.M., Karsch, F.J., 1993. Distribution of estrogen receptor-immunoreactive cells in the sheep brain. Endocrinology 133, 876–886. https://doi.org/10.1210/endo.133.2.8344223.
Liu, X., Zhu, X.-H., Zhang, Y., Chen, W., 2013. The change of functional connectivity specificity in rats under various anesthesia levels and its neural origin. Brain Topogr. 26, 363–377. https://doi.org/10.1007/s10548-012-0267-5.
Lotze, M., Domin, M., Gerlach, F.H., Gaser, C., Lueders, E., Schmidt, C.O., Neumann, N., 2019. Novel findings from 2,838 adult brains on sex differences in gray matter brain volume. Sci. Rep. 9, 1671. https://doi.org/10.1038/s41598-018-38239-2.
Makris, N., Swaab, D.F., van der Kouwe, A., Abbs, B., Boriel, D., Handa, R.J., Tobet, S., Goldstein, J.M., 2013. Volumetric parcellation methodology of the human hypothalamus in neuroimaging: normative data and sex differences. NeuroImage 69, 1–10. https://doi.org/10.1016/j.neuroimage.2012.12.008.
McCarthy, M.M., Konkle, A.T.M., 2005. When is a sex difference not a sex difference? Front. Neuroendocrinol. 26, 85–102. https://doi.org/10.1016/j.yfrne.2005.06.001.
McCarthy, M.M., Pickett, L.A., VanRyzin, J.W., Kight, K.E., 2015. Surprising origins of sex differences in the brain. Horm. Behav. 76, 3–10. https://doi.org/10.1016/j.yhbeh.2015.04.013.
Meyer, C.E., Kurth, F., Lepore, S., Gao, J.L., Johnsonbaugh, H., Oberoi, M.R., Sawiak, S.J., MacKenzie-Graham, A., 2017. In vivo magnetic resonance images reveal neuroanatomical sex differences through the application of voxel-based morphometry in C57BL/6 mice. NeuroImage 163, 197–205. https://doi.org/10.1016/j.neuroimage.2017.09.027.
Miller, L.R., Marks, C., Becker, J.B., Hurn, P.D., Chen, W.-J., Woodruff, T., McCarthy, M.M., Sohrabji, F., Schiebinger, L., Wetherington, C.L., Makris, S., Arnold, A.P., Einstein, G., Miller, V.M., Sandberg, K., Maier, S., Cornelison, T.L., Clayton, J.A., 2017. Considering sex as a biological variable in preclinical research. FASEB J. 31, 29–34. https://doi.org/10.1096/fj.201600781R.
Molina, A., Moyano, M., Serrano-Rodriguez, J., Ayala, N., Lora, A., Serrano-Caballero, J., 2016. Analyses of anaesthesia with ketamine combined with different sedatives in rats. Vet. Med. 60, 368–375. https://doi.org/10.1721/8384-VETMED.
Nuruddin, S., Bruchhage, M., Ropstad, E., Krogenæs, A., Evans, N.P., Robinson, J.E., Endestad, T., Westlye, L.T., Madison, C., Haraldsen, I.R.H., 2013. Effects of peripubertal gonadotropin-releasing hormone agonist on brain development in sheep—a magnetic resonance imaging study. Psychoneuroendocrinology 38, 1994–2002. https://doi.org/10.1016/j.psyneuen.2013.03.009.
Paasonen, J., Stenroos, P., Salo, R.A., Kiviniemi, V., Gröhn, O., 2018. Functional connectivity under six anesthesia protocols and the awake condition in rat brain. NeuroImage 172, 9–20. https://doi.org/10.1016/j.neuroimage.2018.01.014.
Pecina, H.I., Pecina, T.C., Vyroubal, V., Kruljac, I., Slaus, M., 2017. Age and sex related differences in normal pituitary gland and fossa volumes. Front. Biosci. Elite Ed. 9, 204–213.
Perkins, A., Fitzgerald, J.A., Moss, G.E., 1995. A comparison of LH secretion and brain estradiol receptors in heterosexual and homosexual rams and female sheep. Horm. Behav. 29, 31–41. https://doi.org/10.1006/hbeh.1995.1003.
Perkins, A., Roselli, C.E., 2007. The ram as a model for behavioral neuroendocrinology. Horm. Behav. 52, 70–77. https://doi.org/10.1016/j.yhbeh.2007.03.016.
Polkowska, J., Dubois, M.P., Domański, E., 1980. Immunocytochemistry of luteinizing hormone releasing hormone (LHRH) in the sheep hypothalamus during variuos reproductive stages: correlation with the gonadotropic hormones of the pituitary. Cell Tissue Res. 208, 327–341. https://doi.org/10.1007/BF00234880.
Robinson, J.E., Forsdike, R.A., Taylor, J.A., 1999. In utero exposure of female lambs to testosterone reduces the sensitivity of the gonadotropin-releasing hormone neuronal network to inhibition by progesterone. Endocrinology 140, 5797–5805. https://doi.org/10.1210/endo.140.12.7205.
Roselli, C.E., Larkin, K., Resko, J.A., Stellflug, J.N., Stormshak, F., 2004. The volume of a sexually dimorphic nucleus in the ovine medial preoptic area/anterior hypothalamus varies with sexual partner preference. Endocrinology 145, 478–483. https://doi.org/10.1210/en.2003-1098.
Roselli, C.E., Reddy, R.C., Kaufman, K.R., 2011. The development of male-oriented behavior in rams. Front. Neuroendocrinol. 32, 164–169. https://doi.org/10.1016/j.yfrne.2010.12.007.
Roselli, C.E., Stormshak, F., 2010. The ovine sexually dimorphic nucleus, aromatase, and sexual partner preferences in sheep. J. Steroid Biochem. Mol. Biol. 118, 252–256. https://doi.org/10.1016/j.jsbmb.2009.10.009.
Roselli, Charles E., Stormshak, F., 2009a. The neurobiology of sexual partner preferences in rams. Horm. Behav. 55, 611–620. https://doi.org/10.1016/j.yhbeh.2009.03.013.
Roselli, C.E., Stormshak, F., 2009b. Prenatal programming of sexual partner preference: the ram model. J. Neuroendocrinol. 21, 359–364. https://doi.org/10.1111/j.1365-2826.2009.01828.x.
Roselli, C.E., Stormshak, F., Resko, J.A., 2000. Distribution of aromatase mRNA in the ram hypothalamus: an in situ hybridization study. J. Neuroendocrinol. 12, 656–664. https://doi.org/10.1046/j.1365-2826.2000.00496.x.
Roselli, C.E., Stormshak, F., Resko, J.A., 1998. Distribution and regulation of aromatase activity in the ram hypothalamus and amygdala. Brain Res. 811, 105–110. https://doi.org/10.1016/S0006-8993(98)00995-0.
Rubinov, M., Sporns, O., 2010. Complex network measures of brain connectivity: uses and interpretations. NeuroImage Comput. Models Brain 52, 1059–1069. https://doi.org/10.1016/j.neuroimage.2009.10.003.
Sadeghi, L., Rizvanov, A.A., Salafutdinov, I.I., Dabirmanesh, B., Sayyah, M., Fathollahi, Y., Khajeh, K., 2017. Hippocampal asymmetry: differences in the left and right hippocampus proteome in the rat model of temporal lobe epilepsy. J. Proteom. 154, 22–29. https://doi.org/10.1016/j.jprot.2016.11.023.
Samara, A., Vougas, K., Papadopoulou, A., Anastasiadou, E., Baloyanni, N., Chrousos, G.P., Tsangaris, G.T., 2011. Proteomics reveal rat hippocampal lateral asymmetry. Hippocampus 21, 108–119. https://doi.org/10.1002/hipo.20727.
Sawiak, S.J., Picq, J.-L., Dhenain, M., 2014. Voxel-based morphometry analyses of in vivo MRI in the aging mouse lemur primate. Front. Aging Neurosci. 6. https://doi.org/10.3389/fnagi.2014.00082.
Sawiak, S.J., Wood, N.I., Williams, G.B., Morton, A.J., Carpenter, T.A., 2009. SPMMouse: a new toolbox for SPM in the animal brain. Presented at the ISMRM 17th Scientific Meeting & Exhibition, April 18–24.
Sumiyoshi, A., Nonaka, H., Kawashima, R., 2017. Sexual differentiation of the adolescent rat brain: a longitudinal voxel-based morphometry study. Neurosci. Lett. 642, 168–173. https://doi.org/10.1016/j.neulet.2016.12.023.
Swaab, D.F., Gooren, L.J., Hofman, M.A., 1992. The human hypothalamus in relation to gender and sexual orientation. Prog. Brain Res. 93, 205–217. https://doi.org/10.1016/S0079-6123(08)64573-2. discussion 217-219.
Xia, M., Wang, J., He, Y., 2013. BrainNet Viewer: a network visualization tool for human brain connectomics. PLoS One 8, e68910. https://doi.org/10.1371/journal.pone.0068910.
Zalesky, A., Fornito, A., Bullmore, E.T., 2010. Network-based statistic: identifying differences in brain networks. NeuroImage 53, 1197–1207. https://doi.org/10.1016/j.neuroimage.2010.06.041.